

Designing of a Non-Zero Dispersion Shifted Fiber with Ultra-High Birefringence and High Non-Linearity

Shabbir Chowdhury, Japatosh Mondal

Abstract—Photonic Crystal Fiber (PCF) uses are no longer limited to telecommunication only rather it is now used for many sensors-based fiber optics application, medical science, space application and so on. In this paper, the authors have proposed a microstructure PCF that is designed by using Finite Element Method (FEM) based software. Besides designing, authors have discussed the necessity of the characteristics that it poses for some specified applications because it is not possible to have all good characteristics from a single PCF. Proposed PCF shows the property of ultra-high birefringence (0.0262 at 1550 nm) which is more useful for sensor based on fiber optics. The non-linearity of this fiber is $50.86 \text{ w}^{-1}\text{km}^{-1}$ at 1550 nm wavelength which is very high to guide the light through the core tightly. For Perfectly Matched Boundary Layer (PML), $0.6 \mu\text{m}$ diameter is taken. This design will offer the characteristics of Nonzero-Dispersion-Shifted Fiber (NZ-DSF) for 450 nm waveband. Since it is a software-based design and no practical evaluation has made, 2% tolerance is checked and the authors have found very small variation of the characteristics.

Keywords—Chromatic dispersion, birefringence, NZ-DSF, FEM, non-linear coefficient, DCF, waveband.

I. INTRODUCTION

PCF is the media to convey guided information in the form of light using Total Internal Reflection (TIR) method. For having freedom from electrical interference and possessing signal security, little maintenance requirement, PCF is now more popular than the conventional optical fiber. Generally, fused silica is used as core which is fenced by a systematic arrangement of air holes over the fiber span [1]. It is very much possible to achieve high birefringence [2], high non-linearity [3], controlled operation [4], large chromatic dispersion [5] and large mode area [6] by tailoring air hole diameter and hole-to-hole distance which is inconvenient in conventional fibers.

Birefringence is the difference between the refractive index of the faster and slower axis. When a light ray propagates through the PCF, the birefringent property makes different velocity of o-ray and e-ray, so removing of e-ray becomes easier. This property makes that ray linearly polarized. Using o-ray and e-ray, it is possible to have polarization-maintaining property. High birefringent PCF has become very popular for

polarization maintaining properties and this property is suitable for application of sensor based on optical fiber like temperature-insensitive polarimetric vibration sensor [7], sensor for lateral pressure monitoring applications [8], seawater temperature measurement [9] and so on. High birefringence can be achieved by increasing the asymmetry of the PCF.

When a light pulse propagates through the PCF, the greater frequency travels faster than the lower frequency that causes waveguide dispersion. On the other hand, light interaction with particles of the host material causes material dispersion. Interestingly in PCF, material and waveguide dispersion are off the opposite sign, so proper design can cancel each other out that make it possible to get zero dispersion, near-zero dispersion and NZ-DSF. The term Chromatic Dispersion (CD) is the combination of the material and waveguide dispersion. In PCF, this CD can be made negative to cancel out the positive dispersion of the conventional optical fiber. But some factors such as dispersion compensation ratio, fiber bandwidth, fiber mode property should be kept in mind when a fiber is being designed.

A microstructure PCF is designed in this paper which offers high negative CD and also high non-linearity to guide the light within fiber core tightly that will reduce footprint and power consumption of numerous optical mechanisms. The non-zero dispersion-shifted property reduces the cross-talk when wavelength division multiplexing (WDM) is used to send multiple signals through a single-mode fiber.

II. DESIGN METHODOLOGY

Fig. 1 illustrates the structure of the proposed design. This is designed by using COMSOL Multiphysics 4.2 which is based on FEM. The fiber is of ring main design consisting of circular air holes of $0.62 \mu\text{m}$ diameter and two ellipses with semi-axis $0.25 \mu\text{m}$ and $0.85 \mu\text{m}$, both are located at $0.6 \mu\text{m}$ distances from the center of the fused silica core. The first ring radius R_1 is $1.5 \mu\text{m}$ and rests of four are as the following manner. $R_{n+1} = (R_n + 0.9) \mu\text{m}$, where $n=1, 2, 3, 4$. The first, second, third, fourth and fifth rings have 12, 18, 24, 30, and 36 circular air holes respectively following the equation; number of hole $N_{n+1} = 12 + 6n$; where $n = 0, 1, 2, 3$ with the same radius. The air holes are arranged at the same angular distance from one another in the same ring. The difference $0.6 \mu\text{m}$ between the last two diameters is used as PML.

Shabbir Chowdhury is conducting his MSc in Biomedical Engineering in King Abdulaziz University, Saudi Arabia (corresponding author, phone: 966-581-321695; e-mail: chowdhuryshabbir99@gmail.com).

Japatosh Mondal is an Assistant Professor in Bangabandhu Sheikh Mujibur Rahman Science and Technology University, Bangladesh, currently doing his PhD in Keio University, Japan.

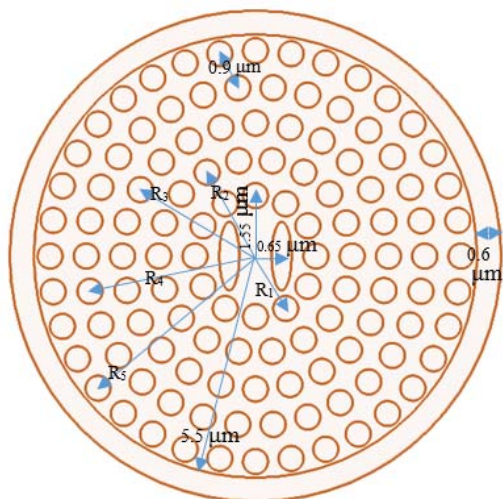


Fig. 1 Cross section of proposed PCF

III. NUMERICAL ANALYSIS METHOD

The birefringence of the PCF is calculated from the variance between the effective refractive indices of x and y axis.

$$B = |n_x - n_y| \quad (1)$$

where, n_x and n_y represent the real parts of x and y axis refractive index respectively. We can have the refractive index from wavelength by using the Sellmeier equation.

Effective area (A_{eff}), CD (D) and nonlinearity (λ) are calculated by:

$$A_{eff} = (\iint |E|^2 dx dy) / \iint |E|^4 dx dy \quad (2)$$

$$D = -\lambda / c \cdot d^2 \text{Re}(n_{eff}) / dy^2 \quad (3)$$

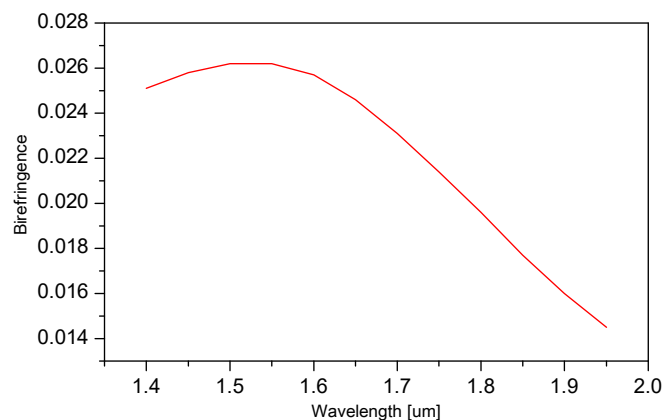
$$\gamma = 2\pi n_2 / (\lambda A_{eff}) \quad (4)$$

where c is the light velocity in vacuum, λ is the wavelength and n_2 is the nonlinear refractive index of fused silica.

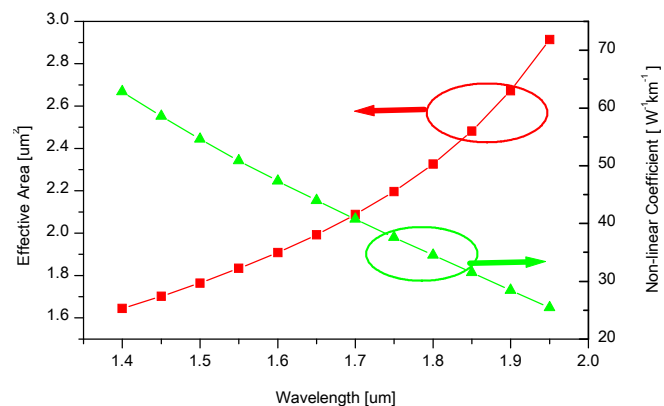
IV. RESULT

Fig. 2 represents the proposed PCF's property where Fig. 2 (a) shows birefringence changes with respect to wavelength variation. The birefringence at 1550 nm wavelength is 0.0262 and it remains greater than 0.0235 for C, L, U wavebands. This high birefringence [10] characteristic makes the fiber useful for sensor application where light is maintained a linear polarization state [11], [12]. Fig. 2 (b) shows the effective area and non-linear coefficients. The effective area and fiber non-linear coefficient at 1550 nm wavelength are 1.8331 and 50.86 respectively. The larger wavelength takes more area of the PCF and from (4) it is known that effective area and fiber non-linearity are inversely proportional to each other. The small effective area [13], [14] will strongly guide the light through

the core and reduce bending loss [11] and other effects of external disturbances. This non-linearity is very high compared to other published papers which are shown at Table I.



(a) Wavelength Vs Birefringence



(b) Wavelength Vs Effective area and Non-linear co-efficient

Fig. 2 PCF property

If dispersion is considered to vary with wavelength linearly in a multi-wavelength channel transmission system, then some dispersion must present in the fiber after compensating the dispersion. This lasting dispersion is known as the residual dispersion which is shown in Fig. 3 (a) that also represents the relation between wavelength and CD. At 1550 nm wavelength, the CD is -373.85 ps/(nm-km) and it increases negatively as wavelength increases. Generally, CD affects the bit error rate and also limits the maximum transmission distance [15]. In that sense, our design provides NZ-DSF as well as highly negative CD to enlarge the transmission efficiency [16]. Moreover, this high negative CD enables the fiber to use as the dispersion compensating fiber (DCF). Fig. 3 (b) represents the relative dispersion slope (RDS) of the proposed PCF.

Fig. 4 represents the effective dispersion of the proposed PCF when it is used as DCF. Fig. 4 (a) shows that there is ± 3.64 ps/nm-km dispersion variation within the wavelength of 1400 nm to 1950 nm and only ± 0.85 ps/nm-km for 1490 nm to 1870 nm [17], [18]. So, this fiber can be used as a DCF and

NZ-DSF for WDM. The RDS of the proposed PCF is 0.002615 at 1550 nm which is shown in Fig. 3 (b).

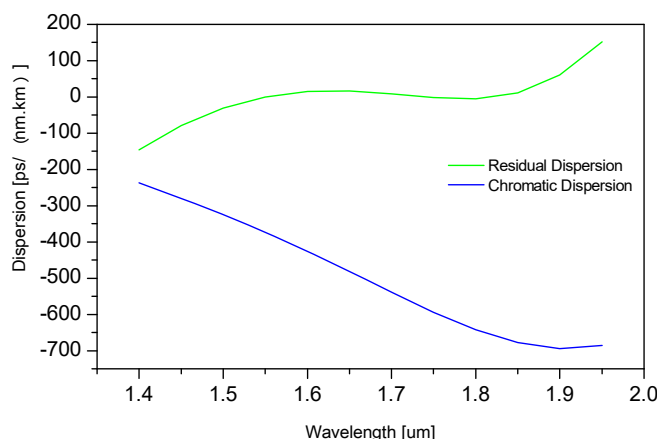


Fig. 3 (a) Wavelength Vs CD and Residual Dispersion

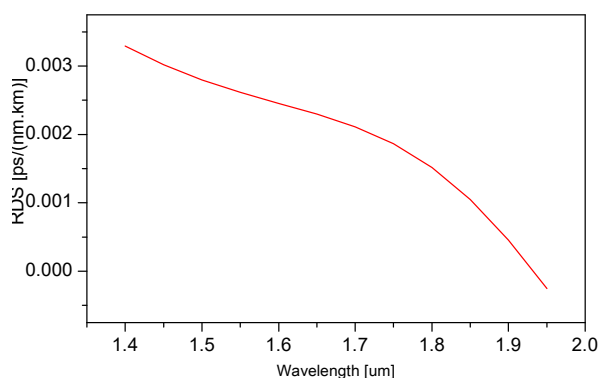


Fig. 3 (b) Wavelength Vs RDS

The property that the proposed PCF possess is compared with some proposed PCF designs that are illustrated in Table I. Moreover, compared PCF design consists of different air filling factors that are the same in our design.

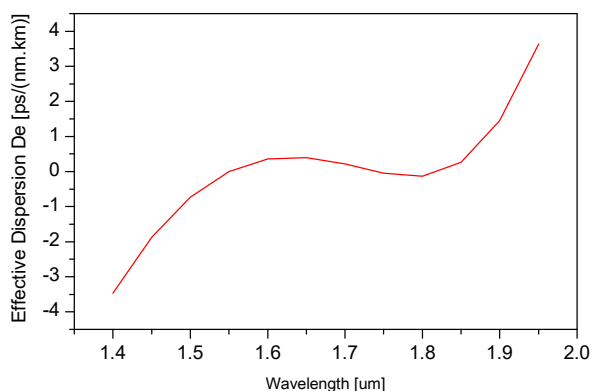


Fig. 4 (a) Wavelength Vs RDS

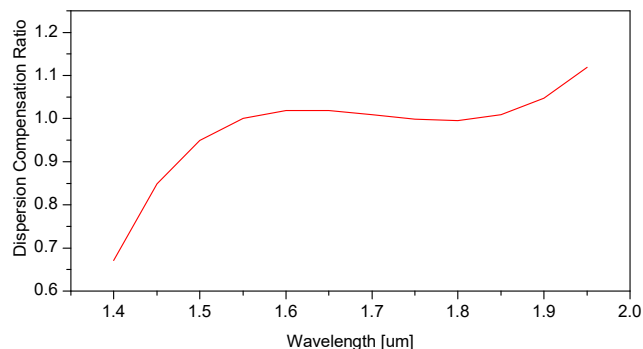


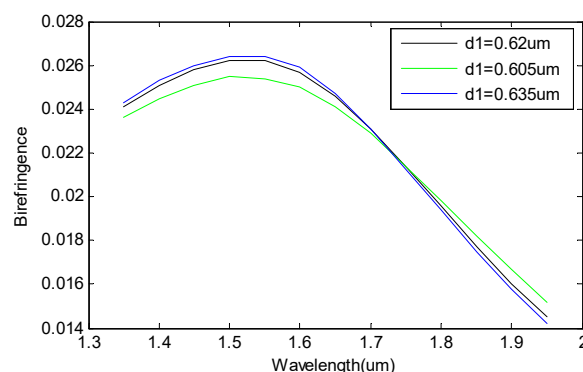
Fig. 4 (b) Wavelength Vs Dispersion Compensating Ratio

TABLE I
 COMPARISON BETWEEN THE PROPOSED PCF AND OTHER PCFS AT 1550 NM

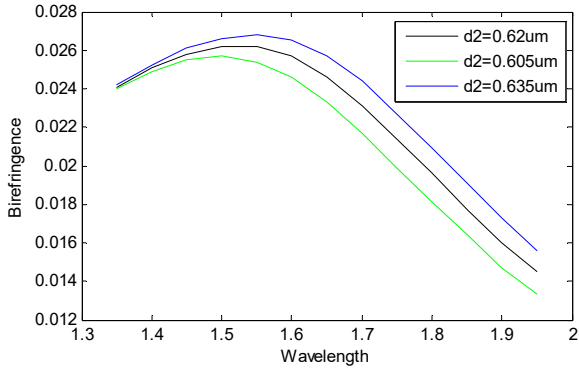
PCF Design	Birefringence B	Non-linear Coefficient $\gamma (w^{-1}km^{-1})$
Ref [10]	1.75×10^{-2}	39.933
Ref [19]	4.2×10^{-2}	-----
Ref [20]	6×10^{-2}	-----
Proposed PCF	2.62×10^{-2}	50.86

V.EFFECT OF PARAMETER VARIATION

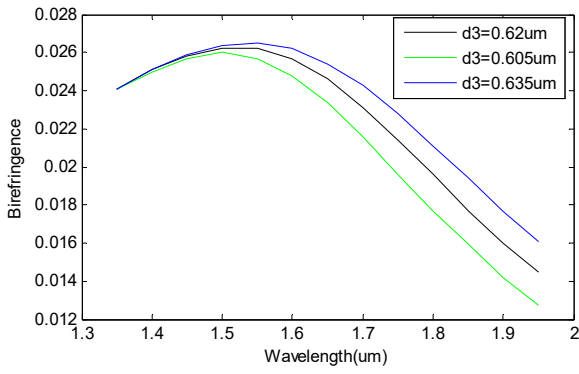
It is not possible to fabricate a PCF that is originally designed. So, parameter is varied while simulation is done to determine the fiber characteristics. In Fig. 5, diameter of circular air hole effect on fiber birefringence is shown. In Fig. 5 (a) $d_1 = 0.62 \pm 0.015 \mu m$ and $d_2 = d_3 = d_4 = d_5 = 0.62 \mu m$, (b) $d_2 = 0.62 \pm 0.015 \mu m$ and $d_1 = d_3 = d_4 = d_5 = 0.62 \mu m$, (c) $d_3 = 0.62 \pm 0.015 \mu m$ and $d_1 = d_2 = d_4 = d_5 = 0.62 \mu m$, (d) $d_4 = 0.62 \pm 0.015 \mu m$ and $d_1 = d_2 = d_3 = d_5 = 0.62 \mu m$. Here d_1, d_2, d_3, d_4, d_5 are the circular air hole diameters of 1st, 2nd, 3rd, 4th and 5th ring. It is found that there is almost no effect of first ring air hole diameter variation on Birefringence. For second and third ring's air hole diameter variation, birefringence is varied but very little and is still usable for polarization-maintaining fiber. Dependence of birefringence on hole diameter is minimized for succeeding rings.



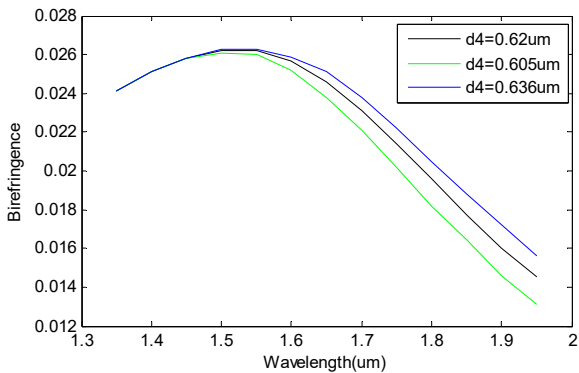
(a)



(b)



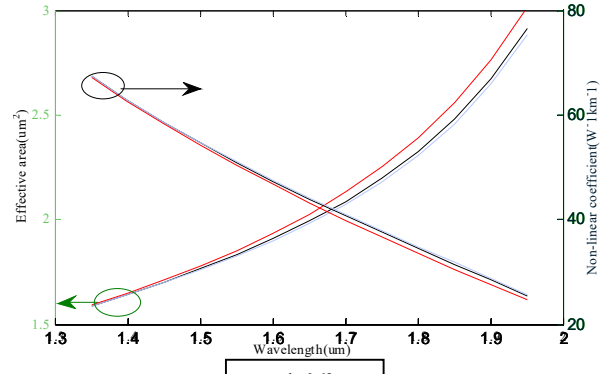
(c)



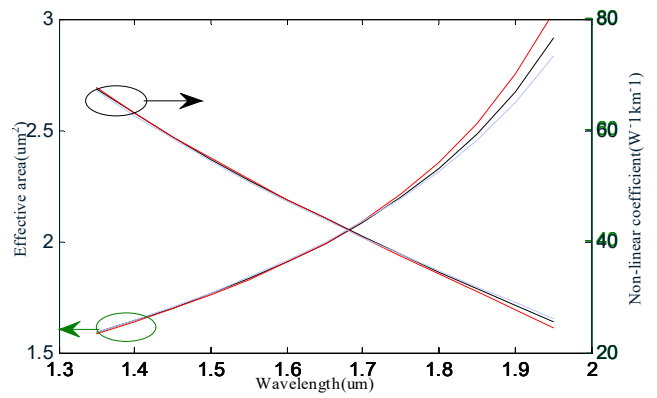
(d)

Fig. 5 Effect of air hole diameter variation on birefringence

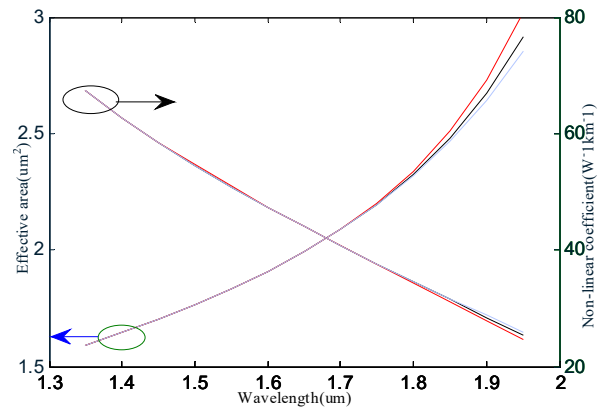
In Fig. 6, the effect of air hole diameter variation on fiber effective area and non-linearity is demonstrated. In Fig. 6 (a) $d_1 = 0.62 \pm 0.015 \mu\text{m}$ and $d_2 = d_3 = d_4 = d_5 = 0.62 \mu\text{m}$, (b) $d_2 = 0.62 \pm 0.015 \mu\text{m}$ and $d_1 = d_3 = d_4 = d_5 = 0.62 \mu\text{m}$, (c) $d_3 = 0.62 \pm 0.015 \mu\text{m}$ and $d_1 = d_2 = d_4 = d_5 = 0.62 \mu\text{m}$, (d) $d_4 = 0.62 \pm 0.015 \mu\text{m}$ and $d_1 = d_2 = d_3 = d_5 = 0.62 \mu\text{m}$. It is found that though the first ring air hole diameter change has very little effect on area and non-linearity, rest of the air hole diameter variation has no effect on them for fiber operating wavelengths.



(a)



(b)



(c)

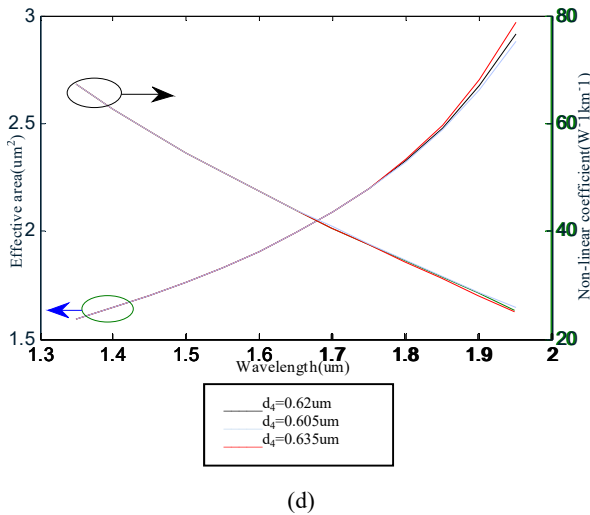
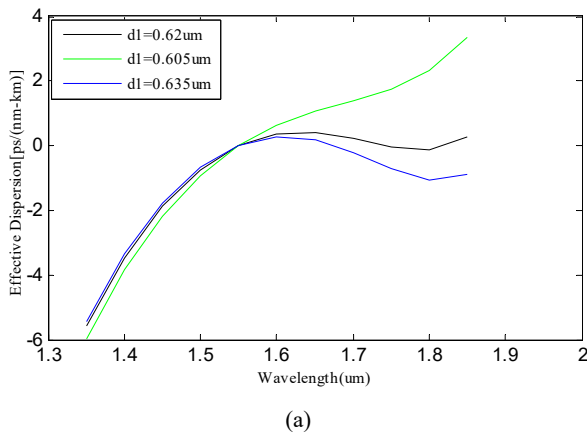


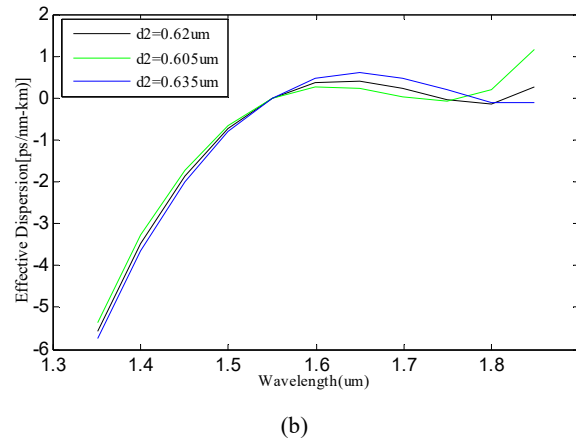
Fig. 6 Effect of air hole diameter variation on effective area and non-linearity

Fig. 7 shows the dispersion phenomena of the proposed PCF where the diameter of circular air holes is varied. It is seen in Fig. 7 (a) that the first ring's air hole has more effect on the dispersion, so care should be taken to variation of first ring's air holes. But the second ring's air hole diameter variation has a very negligible effect on dispersion phenomena (shown in Fig. 7 (b)). Though dispersion dependence on the air hole diameter increases for the third ring (shown in Fig. 7 (c)), it further decreases from the fourth ring (shown in Fig. 7 (d)).

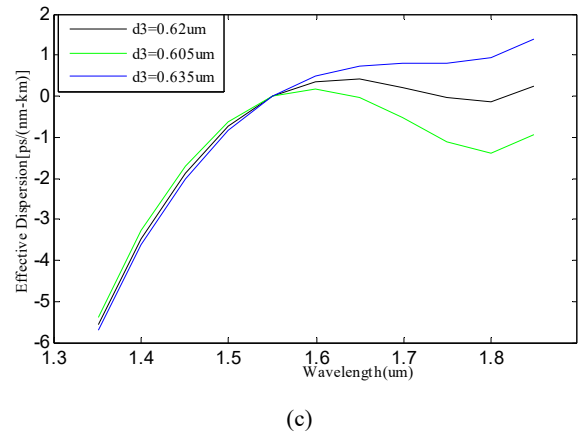
The elliptical air holes are mainly included for higher birefringence and nonlinearity. The effect of elliptical air hole size variation is shown in Fig. 8. In Fig. 8 (a) birefringence variation for 1% change in both two semi-axis of ellipses, (b) dispersion variation for 1% change in two semi-axis of ellipses, (c) non-linearity variation for 1% change in two semi-axis of ellipses are shown. It is seen from Fig. 8 that elliptical air holes having semi-axis 0.25 ± 0.0025 and 0.85 ± 0.0085 have very little effect on the fiber characteristics which strengthens the fiber design for practical applications.



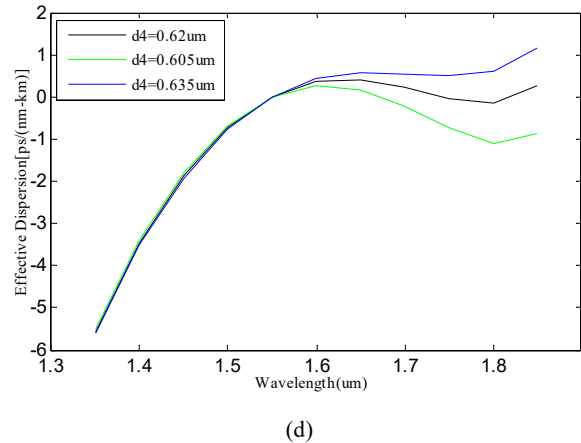
(a)



(b)



(c)



(d)

Fig. 7 Effect of air hole diameter variation on dispersion

Confinement loss is defined as the inability of optical fiber to confine light in it. In case of our designed PCF, confinement loss is larger but it can be reduced very easily by increasing the number of air holes. The more the air hole placed on the silica the lesser will be the confinement loss. This is shown in Fig. 9 where an increasing the number of rings (NR) decreases the confinement loss. Every two new air hole rings decrease more than ten orders of the previous loss. At 1550 nm wavelength, confinement loss becomes zero for nine air rings of air holes whereas it was $(1.0e + 006) \times 0.0074$ dB/km for five rings. For five rings, the number of circular air

hole is 12, 18, 24, 30, 36 respectively. For seven rings, the numbers of circular air holes are on the order of 12, 18, 24, 30, 36, 45, 45. And for nine rings, they are placed on the order of 12, 18, 24, 30, 36, 45, 45, 60, 60. So it is possible to have very low confinement loss by adding new air rings consisting of circular air holes.

VI. TOLERANCE

The tolerance of the proposed fiber is checked and the result is shown in Fig. 10. For this tolerance check, the diameter of all circular air holes and pitch are varied 2% from the proposed design. So, for +2% tolerance check, the diameter of all circular air holes is 0.6324 and the pitch is 0.91 whereas the diameter of -2% tolerance check is 0.6076 and pitch is 0.882. In Fig. 10 (a) birefringence variation for $\pm 2\%$ parameter change, (b) Effective area and non-linearity variation for $\pm 2\%$ parameter change, (c) dispersion variation for $\pm 2\%$ parameter change are shown respectively.

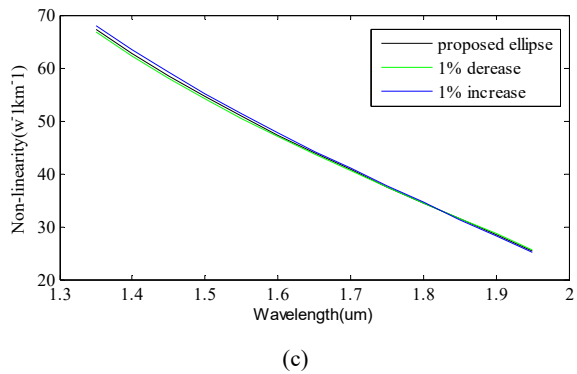
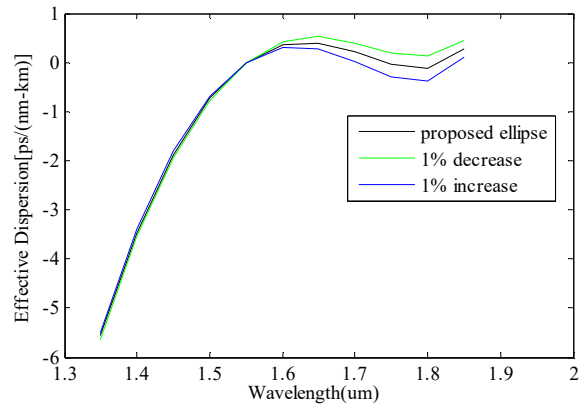
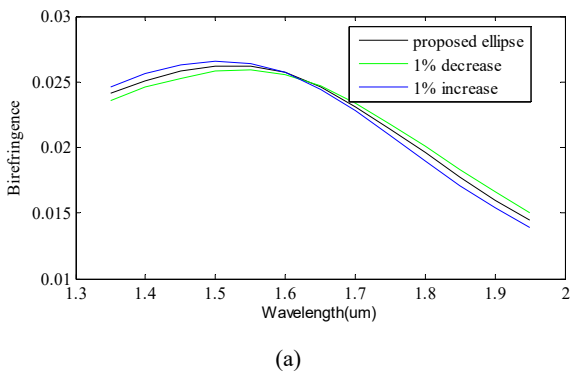


Fig. 8 Effect of ellipse size on Birefringence, Dispersion and Non-linearity

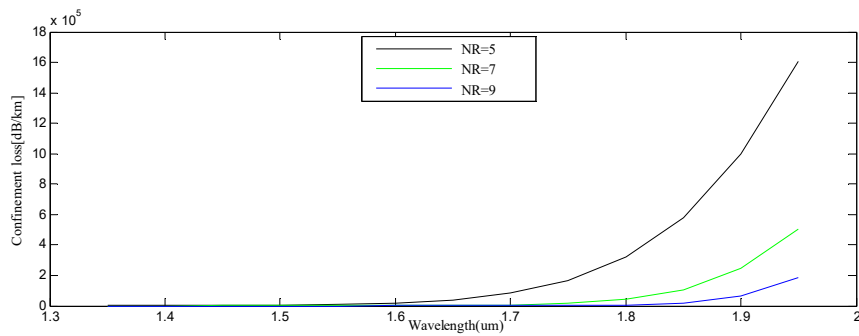
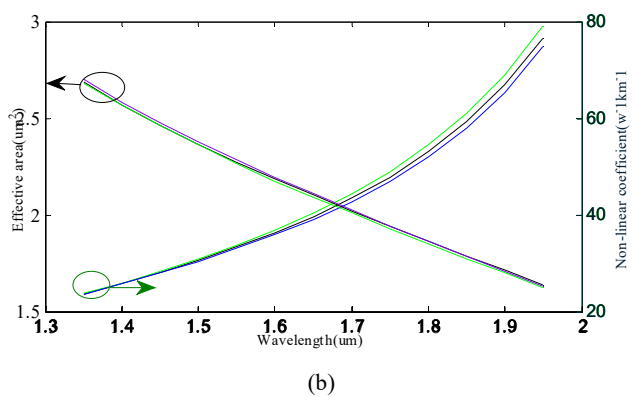
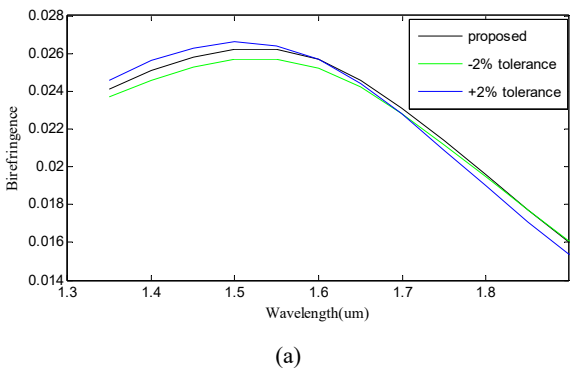


Fig. 9 Effect of air hole rings on confinement loss



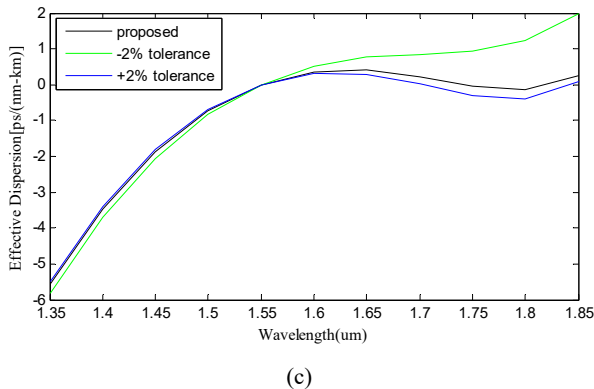


Fig. 10 Tolerance check of the proposed PCF

VII. CONCLUSION

The proposed design is of ultra-high birefringence PCF having more advantages as compared to the recently proposed designs. The birefringence property of the proposed design is good enough to use it in many sensors based optical applications. It is greater than 0.024 for S+C+L+U wavebands, high negative CD makes it usable as DCF. With a small effective area, the fiber offers more than $40 \text{ w}^{-1}\text{km}^{-1}$ non-linear coefficients for S+C+L+U wavebands. Moreover, the effective dispersion is only $\pm 0.6 \text{ ps}/(\text{nm}\cdot\text{km})$ for 1525 nm to 1850 nm wavelength. In summary, a fixed diameter to pitch ratio (0.689) makes this design worthy of practical implementation whereas confinement loss will be minimized in our future work.

REFERENCES

- [1] P. Russell, "Photonic-Crystal Fibers", J. Lightwave Technol., vol. 24, pp. 4729-4749, 2006.
- [2] J. F. Liao and J. Q. Sun, "High birefringent rectangular-lattice photonic crystal fibers with low confinement loss employing different sizes of elliptical air holes in the cladding and the core," Opt. Fiber Technol., vol. 18, no. 6, pp. 457-461, Dec. 2012.
- [3] Jianfei Liao, Junqiang Sun, Mingdi Du, and Yi Qin, "Highly nonlinear dispersion-flattened slotted spiral photonic crystal fibers," IEEE Photonics Technology Letters, vol. 26, no. 4, Feb. 2014.
- [4] J. C. Knight, J. Arriaga, T. A. Birks, et.al., "Anomalous dispersion in photonic crystal fiber", IEEE Photonics Technology Lett., vol. 12, pp.807-809, 2000.
- [5] M. A. Islam and M. S. Alam, "Design of a polarization-maintaining equiangular spiral photonic crystal fiber for residual dispersion compensation over E + S + C + L + U wavelength bands," IEEE Photon. Technol. Lett. vol. 24, no. 11, pp. 930-932, Jun. 1, 2012.
- [6] J. C. Knight, T. A. Birks, R. F. Cregan, P. St. I. Russell, and I.-P. de Sandro, "Large mode area photonic crystal fibre," Electron. Lett., vol. 34, no. 13, pp. 1347-1348, Jun. 1998.
- [7] Karima Chah, et.al, "Temperature-insensitive polarimetric vibration sensor based on HiBi microstructured optical fiber", Applied Optics, Vol. 51, No. 25, 1 September 2012.
- [8] Mohammad Karimi, Tong Sun, and Kenneth. T. V. Grattan, "Design evaluation of a high birefringence single mode optical fiber-based sensor for lateral pressure monitoring applications" IEEE Sensors Journal, VOL. 13, NO. 11, November 2013.
- [9] Xin Wang, Hong-Juan Yang, Shan-Shan Wang, Yi-Peng Liao, and Jing Wang, "Seawater temperature measurement based on a high birefringence elliptic fiber sagnac loop" IEEE Photonics Technology Letters, VOL. 27, NO. 16, August 15, 2015.
- [10] Japatoosh Mondal, Mohammad Shaifur Rahman, " Design of highly birefringent dispersion compensating spiral photonic crystal fiber" in 2nd Int'l Conf on Electrical Engineering and Information &

- Communication Technology (ICEEICT) 2015, Bangladesh, 2015, ©2015 IEEE, DOI: 10.1109/ICEEICT.2015.7307515.
- [11] H. Ademgil, S. Haxha, T. Gorman, and F. AbdelMalek, "Bending effects on highly birefringent photonic crystal fibers with low chromatic dispersion and low confinement losses" Journal of Lightwave Technology, VOL. 27, NO. 5, March 1, 2009.
- [12] Lin An, Zheng Zheng, Zheng Li, Tao Zhou, and Jiangtao Cheng, "Ultrahigh birefringent photonic crystal fiber with ultralow confinement loss using four airholes in the core" Journal Of Lightwave Technology, VOL. 27, NO. 15, August 1, 2009.
- [13] N. A. Mortensen, "Effective area of photonic crystal fibers," Opt. Exp., vol. 10, pp. 341-348, 2002.
- [14] N. A. Mortensen and J. R. Folkenberg, "Low-loss criterion and effective area considerations for photonic crystal fibers," Journal of Optics A: Pure And Applied Optics vol. 5, pp. 163-16, 2003.
- [15] Graham H. Smith, Dalma Novak, and Zaheer Ahmed, "Overcoming chromatic-dispersion effects in fiber-wireless systems incorporating external modulators", IEEE Transactions on Microwave Theory and Techniques, Vol. 45, No. 8, August 1997.
- [16] P. S. Andre I, A. L. J. Teixeira, M. Lima, J. F. da Rocha, J. L. Pinto, "Nonlinear refractive index and chromatic dispersion simultaneous measurement in non-zero dispersion shift optical fibres", 4th International Conference on Transparent Optical Networks, warsaw poland 2002, vol.1, pp. 111 - 114, 2002.
- [17] Franco, M. A., Serrão, V. A., & Sircilli, F. Microstructured optical fiber for residual dispersion compensation over wavelength bands. IEEE Photonics Technology Letters, 20(9), pp. 751-753, 2008.
- [18] Habib, M. S., Haque, M. M., Habib, M. S., Hasan, M. I., Rahman, M. S., & Razzak, S. M. A., Polarization maintaining holey fibers for residual dispersion compensation over S+ C+ L wavelength bands. Optik-International Journal for Light and Electron Optics, 125(3), pp. 911-915, 2004.
- [19] T. I. Yang, et.al, "High birefringence and low loss circular air-holes photonic crystal fiber using complex unit cells in cladding", Opt. Comm., vol. 281, pp. 4334-4338, 2008.
- [20] Russel Reza Mahmud; Muhammad Abdul Goffar Khan; S. M. Abdur Razzak "Design and Analysis of a new photonic Crystal Fiber for Fiber Based Sensor Applications", 2015 IEEE International Conference on Telecommunications and Photonics (ICTP), ©2015 IEEE, DOI: 10.1109/ICTP.2015.7427933.